Nuclear and Emerging Technologies for Space, American Nuclear Society Topical Meeting
Richland, WA, February 25 – February 28, 2019, available online at http://anstd.ans.org/

TRADES ON DENSIFIED PROPELLANT FOR NUCLEAR THERMAL PROPULSION

Alexander Aueron[1], Dr. Dale Thomas[1]

[1]301 Sparkman Drive, Huntsville, Alabama, 35899

Nuclear Thermal Propulsion is an enabling technology for expanding both manned and unmanned spaceflight capability. For most efficient use of propellant by mass it must use cryogenic hydrogen, but its mass density is low compared to other propellant options. This results in large propellant tanks which can be heavy and absorb more heat from the space environment than smaller propellant tanks. Hydrogen's density can be increased by storing it at lower temperatures, but such densification is usually discussed in the context of launch vehicles or other Earth applications. This paper explores trades on in space liquid hydrogen propellant storage that result from densified liquid hydrogen. It was found that during spacecraft coast storing close to the freezing point results in a small reduction of required active cooling power compared to storing near the boiling point. During burns when the Nuclear Thermal Propulsion emits neutrons and gamma rays increased liquid hydrogen density increases the amount of heat absorbed from the radiation per unit area and depth of hydrogen, but the higher density allows for more favorable tank geometries that reduce net heating.

I. Introduction

I.A. Nuclear Thermal Propulsion History

Development of Nuclear Thermal Propulsion (NTP) started in America with the Nuclear Engine for Rocket Vehicle Application (NERVA) program in 1947. Initially a United States Air Force intercontinental ballistic missile program, it was taken over by NASA for use in space exploration in 1958 and ran until 1972. Thrust and specific impulse (I_{SP}), which is a propellant mass efficiency metric, achieved during the NERVA program were as high as 890 kN and 835 s respectively, comparable thrust to the Saturn V's J-2 engine 1000 kN of thrust that had only 434 s I_{SP}.[1,2] However, declining public interest in the Apollo program resulted in the decision to cancel Apollo flights 18-20 as well as the post-Apollo program, including NERVA. Renewed interest in Moon and Mars missions starting in 1989 has revived interest in NTP due to its development history and performance.[3]

I.B Liquid Hydrogen in Space

Hydrogen is a high I_{SP} propellant for both chemical and nuclear rockets due to its low molecular weight. Equation (1) is adapted from chemical rocket equations to predict the I_{SP} for a spacecraft using NTP[1]:

$$I_{SP}\ [s] \propto \sqrt{\frac{T\ [k]}{Molecular\ Weight\ of\ Propellant\ \left[\frac{kg}{Kmol}\right]}} \quad (1)$$

The I_{SP} is proportional to the propellant's molecular weight and temperature, making hydrogen the best choice from an I_{SP} perspective. Liquid hydrogen (LH_2) is already used as propellant for chemical launch vehicles today, but to remain a liquid hydrogen must be stored below 20 K at atmospheric pressure. In this launch vehicle application propellant storability is not usually a problem, but long duration spaceflight can provide challenges to cryogenic storage. Launch vehicles can use propellant before it has a chance to boil, but during long term storage too much propellant changing from liquid to vapor can over pressurize tanks.[1] If this happens, the propellant must be vented to avoid bursting the tanks and this wastes that propellant. NASA is developing a 20-watt, 20 K cryocooler for thermal control of space-based LH_2 to prevent boil off of this cold propellant.[4]

I.C Densified Propellant

LH_2's density is a function of storage temperature. The National Institute of Standards and Technology (NIST)'s Chemistry WebBook has a database of LH_2 properties and was used to construct a linear fit of the relationship between LH_2's temperature and density at 1 atm of pressure given by equation (2).

$$\rho(T\ [K]) = -0.97662084 \cdot T\ [K] + 90.88923982 \quad (2)$$

This fit applies from 20.369 K (boiling) to 14 K (slightly above freezing) over which LH_2's density increases from about 71 kg/m^3 to about 77 kg/m^3, an 8.75% increase. Beyond this point, further densification can be achieved by freezing a portion of the LH_2 and this is referred to as slush hydrogen.[5] At the triple point (13.8 K, 0.0695 atm) solid hydrogen has mass density 86.51 kg/m^3, a 12% increase in density compared to 77 kg/m^3 liquid hydrogen at 14 K, but the bulk density will depend on the ratio of solid to liquid hydrogen in the slush.[6]

II. Methodology

Spacecraft that utilize NTP must use LH_2 propellant for their highest possible I_{SP}. As this already requires tackling the challenge of in space cryogenic fluid management, this paper seeks to determine the pros and cons of storing the propellant at even lower temperatures than would be allowed by a 20 K cryocooler. While even greater densities can be achieved by utilizing slush hydrogen, this paper considers just liquid hydrogen so that the tank contents can be assumed to be homogenous. Restricting consideration to the liquid range, simplified propellant tanks were designed for both 20 K storage and 14 K storage of 20 metric tons of LH_2 which were then evaluated on:

- Tank mass (kg)
- Required active cooling heat rejection due to space environment during spacecraft coast (W)
- Heating induced by NTP neutron and gamma radiation during NTP burns (W)

II.A Tank Design

Spacecraft propellant tanks often take the form of spheres or cylinders. Spheres are a beneficial shape as they are the most efficient volume for a given surface area. However, if a sphere cannot contain enough propellant within the volume limits of a launch vehicle payload fairing cylinders are a common choice. For this paper, propellant tank mass is estimated based on the Maximum Expected Operating Pressure (MEOP) and dimensions of a 2219 – Aluminum propellant tank.[1] Cylindrical tanks often have elliptical or spherical end caps, but this paper considers cylinders with flat ends for ease of NTP radiation analysis. For the purpose of this analysis, this slightly reduced the tank surface area which reduces the required tank material. This MEOP is set at 1 atm (101.325 KPa) with a factor of safety of 2, a typical value for pressure vessels.[1] The required thickness of the propellant tank and resulting mass of the tank are calculated by equations (3) through (5).[1]

$$P_{burst} = f_s \cdot MEOP \qquad (3)$$

$$t = P_{burst} \cdot \frac{r}{F_{all}} \qquad (4)$$

$$m = A_{surface} \cdot t \cdot \rho_{tank\ material} \qquad (5)$$

Based on these equations, a tank could be designed for higher pressure storage, but would require a thicker, more massive tank. Also, equation (4) is specifically for the cylindrical section of the propellant tank so does not consider the flat end geometry. From equations (3) through (5), the mass of the propellant tank is proportional to the MEOP so for any given tank geometry the tank will be more massive if a higher MEOP is required of it. A reason one might wish for higher pressure storage is to allow for higher LH_2 storage temperature to ease the burden on active cooling systems. Considering the data on LH_2 boiling point and associated density visualized in figure 1, the associated mass penalty for this design choice comes into focus.

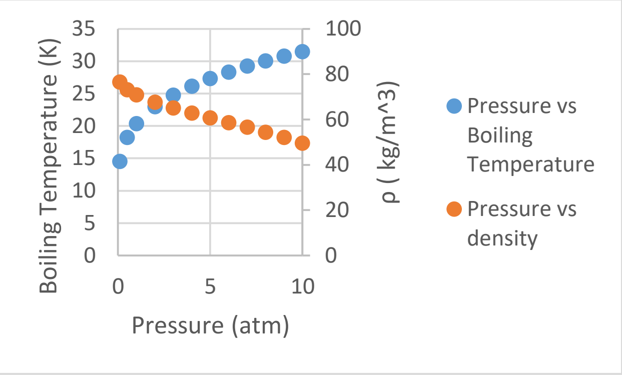

Fig. 1. LH_2 boiling point and density data

$$LH_2\ density \left[\frac{kg}{m^3}\right] = -2.492780748 \cdot P[atm] + 73.887201 \qquad (6)$$

$$LH_2 boiling\ point\ [K] = 20.66319017 \cdot (P[atm])^{0.1772825} \qquad (7)$$

Through visual inspection of figure 1 it is apparent that boiling point does indeed raise with increased pressure, but the associated density of the LH_2 at these boiling points falls with the increased temperature. Equations (6) and (7) are curve fits of the data plotted in figure 1 from which the rates of change can be approximated: -2.5 kg/m^3/atm and 3.66P$^{-0.82}$ K/atm. From these derivatives, there are diminishing returns to increasing the boiling point by increasing pressure, but the decrease in LH_2 density is approximately constant. Therefore, the storage temperature can be increased by increasing the storage pressure, but at the cost of decreased LH_2 density, increasing both the thickness and volume of the tank, driving up tank mass. Constraints imposed by particular active cooling systems will determine optimum storage temperature for a given spacecraft, but in light of this clear mass penalty to high pressure storage this paper focuses on just 1 atm storage. As this paper considered just one tank pressure and material, the differences in tank mass resulted from choice of tank dimensions to accommodate the propellant volume.

II.B Space Environment Thermal Balance

Thermal analysis of the propellant tank was an equilibrium power balance as documented in chapter 11 of Space Mission Analysis and Design. The orbit used for analysis was a 36,000 km altitude circular orbit about the Earth at which albedo and infra-red heating from the Earth are negligible. Emissivity and absorptivity was taken to be 0.005 for MLI of large cryogenic tanks.[7] The propellant tank was assumed to absorb sunlight side-on and reject heat through its entire surface area. The resulting heat balance is equation (8).

$$Q_{passive} + Q_{active} = Q_{sun} \qquad (8)$$

II.C NTP Radiation Heating

NTP produces neutron and gamma radiation during reactor operation and cool down which deposit heat in matter as they are attenuated. Hydrogen in particular is effective at attenuating neutrons so will be heated by neutrons if exposed to them. While less effective at attenuating gamma rays, hydrogen will also be heated as they are attenuated. This radiation transport problem is often solved by Monte Carlo Simulation such as MCNP. In the case of hydrogen propellant this can be modeled with the analytical "Exponential" method which is described in equations (9) through (14).[8]

$$P_{rad} = E_{rad} \cdot \Gamma_{rad} \quad (9)$$

$$P_{rad,F} = P_{rad,I} \cdot e^{-\rho \cdot \sigma \cdot dx} \quad (10)$$

$$\dot{Q}_{rad,N} = \left(P_{rad,I} - P_{rad,F}\right) \quad (11)$$

$$\dot{Q}_{rad,\gamma} = \left(P_{rad,I} - P_{rad,F}\right) \cdot B \cdot \left(1 - \frac{\varepsilon_f}{\varepsilon_i}\right) \quad (12)$$

$$\frac{\varepsilon_f}{\varepsilon_i} = 0.458007 \cdot (\varepsilon_i[MeV])^{-0.4571616} \quad (13)$$

$$B = A_E \cdot e^{(-\alpha \cdot \sigma \cdot \rho \cdot x)} + (1 - A_E) \cdot e^{-\beta \cdot \sigma \cdot \rho \cdot x} \quad (14)$$

As can be seen in the model's equations, the radiation attenuated and resulting heat deposited is a function of the propellant density so there should be an observable impact on NTP radiation heating as a result of changing the propellant density. The change in propellant tank dimensions may also change the total amount of NTP radiation incident on the propellant tank. This effect was included in the radiation analysis by specifying a reactor source of 500 MW at a distance of 5 m from the edge of the propellant tank. The reactor was treated as a point source with internal shielding and the radiation it emitted would experience geometric attenuation as it traveled the 5 m between the reactor and tank. Attenuation by propellant tank wall material was not considered for this analysis.

Cylindrical tanks with flat ends are employed in this modeling effort to simplify implementation of the Exponential method. This choice enables a simplified modeling scenario where all incident radiation travels that same length through the hydrogen whereas if a more realistic spherical end cap were used this would not be the case. Instead, the spherical end cap would cause the radiation that is incident upon the center of the end cap to travel further through hydrogen than radiation incident closer to the edges of the cylindrical section of the tank, adding another dimension to the analysis. Such consideration is a potential future work item, but not considered for this analysis.

III. Results

The tank designs and highlights of the analysis results are listed in Tables I through IV and figures 2 and 3. Design 1 is the baseline tank which stores propellant at 20 K, designs 2 and 3 are two geometries of the same mass of propellant as design 1 but reduced volume due to storage at 14 K. Of particular note are the negligible passive heat rejection of all tank designs. Whether storing at 14 K or 20 K this passive heat rejection capability is dwarfed by the active heat rejection required to maintain the storage temperature in equilibrium (mW vs. W). This active heat rejection required is the majority of the incident heating from sunlight which is why Q_{sun} was omitted from Table II. Both 14 K tank designs had lower active cooling required as a result of their reduced volume, but design 2 had the lowest as its dimensions reduced the area the sunlight was incident upon more than designs 1 and 3. Also of note, the tank masses of designs 2 and 3 are smaller than the mass of design 1 as expected due to the reduced tank dimensions.

TABLE I. Tank Design Properties

Tank Design	Propellant Mass (tons)	T Storage (K)	r (m)	L (m)
1	20	20	3.5	7.3
2	20	14	3.5	6.7
3	20	14	3.4	7.3

TABLE II. Tank Mass, Volume, and Thermal Properties

Tank Design	Tank Mass (kg)	V (m^3)	Q passive (W)	Q active (W)
1	1140.3	280.3	0.011	348.4
2	1081.8	259.0	0.003	322.0
3	1040.5	259.0	0.003	335.0

Just as with the heating due to the space environment there was a reduction in total heat input from NTP radiation as LH_2 density increased and the corresponding tank designs dimensions decreased compared to design 1. This design specific total heating values at documented in Table III. The heat profiles from the radiation in Figures 2 and 3 provide more insight into why the total heating in Table III occurred.

The gamma ray heating profiles are similar for all three tank designs, but the change in density and tank dimensions results in notable differences. Inspecting Figure 2, design 2 has the same end area as design 1 so the same amount of gamma ray power is incident upon both tank designs, but the higher LH_2 density increases the amount of gamma ray power attenuated per unit length of LH_2. This can be seen by the heat deposition profile for design 2 starting at a higher initial value than design 1. This also results in shifting more of the gamma ray induced heating towards the source-side of the tank. Design 2 still has a lower overall gamma induced heating due to the design having a shorter length with which to absorb gamma heat. Design 3 has a similar profile to Design 2, but a smaller tank end area for the gamma rays to be incident upon. This can be seen on figure 2 by design 3's heat deposition profile having a lower initial value than design 2. This results in fewer gamma rays that can be attenuated in design 3 than in design 2. This change in geometry also reduces the total amount of gamma heating in design 3 compared to design 1.

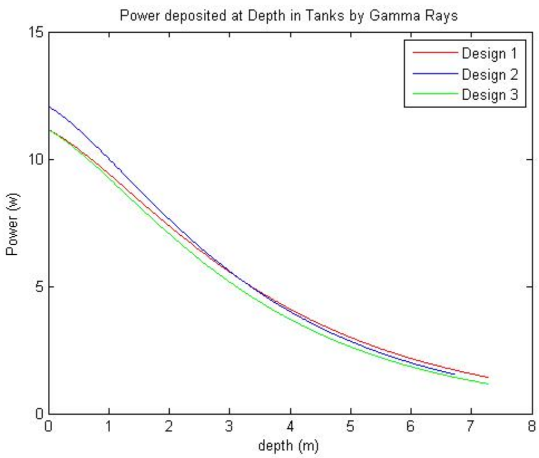

Fig. 2. Gamma Ray heating profiles

As seen in Figure 3 the neutron heating profiles are quite similar for all three tank designs with the majority of neutron radiation attenuating in the first meter of LH_2. However, design 2 has a higher heat deposition than design 1 at the beginning of the LH_2 tank due to the higher LH_2 density attenuating more neutrons in shorter lengths. Design 2 still has a slight overall reduction in neutron heating compared to design 1 due to the smaller tank length catching less of the small amount of remaining neutron radiation. Design 3 has a greater reduction in neutron heating due to the smaller tank end area for radiation to be incident upon.

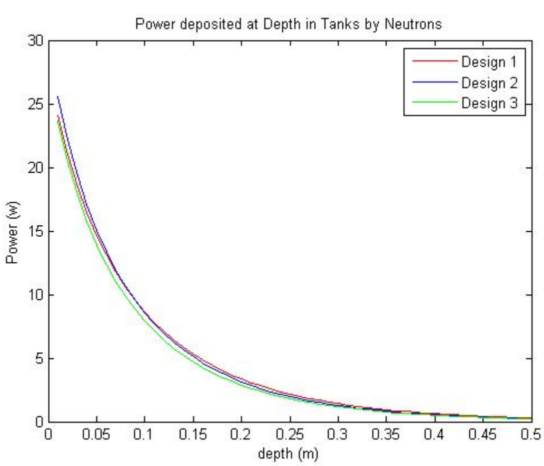

Fig. 3. Neutron heating profiles

TABLE III. NTP Radiation Heating

Tank Design	Total Heating (W)	N Heating (W)	γ Heating (W)
1	4.0709E+03	240	3.8309E+03
2	4.0686E+03	238	3.8307E+03
3	3.8311E+03	220	3.6113E+03

The resulting changes to tank mass and propellant heating are compiled in Table IV. Storing LH_2 at 14 K at 1 atm storage pressure resulted in both reduced net propellant heating and tank mass compared to 20 K storage at 1 atm. The analysis found that the heating from NTP radiation during engine operation was much higher than space environment heating (kW vs. W) at the Earth orbit altitude and spacecraft orientation considered. This resulted in design 2 having a lower active cooling power requirement, but higher NTP radiation induced heating than design 3.

TABLE IV. Results Summary

Tank Design	Net Q (W)	Net Q reduction (W)	Reduction in tank mass (kg)
1	4.42E+03	-	-
2	4.39E+03	28.70	58.5
3	4.17E+03	253.20	99.8

IV. CONCLUSIONS

LH_2 propellant densification offers another option to impact design of spacecraft. In this paper a spacecraft utilizing NTP was considered with both 20 K and 14 K propellant storage to determine impacts to tank design and active cooling requirements. It was determined that lower temperature storage reduces propellant volume, thereby reducing the volume and mass of the propellant tank. This reduced geometry also reduces the amount of incident solar radiation which in turn reduces the total required heat removal by active cooling systems. The change in propellant storage temperature had negligible impact on passive heat rejection capability for the propellant tank.

Spacecraft that utilize NTP must also consider heating induced by the NTP radiation. It was found that higher density LH_2 increases its effectiveness at attenuating both neutrons and gamma rays, but the changes in geometry allowed for the same mass of LH_2 can result in lower overall heating by reducing the amount of incident radiation and the length of hydrogen over which the radiation can attenuate and deposit its heat.

Combining the results of the space environment and induced NTP radiation heating analysis, there is a net benefit to spacecraft design in reduced propellant tank mass and total amount of heat active cooling must reject from increasing LH_2 density. However, this analysis does not consider the details of the cryocoolers required to store

LH_2 at 20 and 14 K. To realize the benefit of storing LH_2 at higher density 14 K cryocoolers must be practical in spaceflight applications. While NASA is currently developing 20 K cryocoolers for in-space use[4], the findings of this study suggest that study of cryocoolers having capability below 20K would be worthwhile since they potentially enable a more optimal spacecraft configuration.

When considering both the space environment thermal situation and the NTP radiation thermal situation the duration of both scenarios must also be considered. The most extreme NTP radiation heating scenario (full power during burns) is a transient scenario while space environment heating persists for the entire mission so will be at or approach equilibrium for much of the mission. Future work on this subject would benefit from transient analysis of NTP radiation heating with a range of LH_2 densities to determine the significance of NTP heating for the relative short burn durations to vehicle design. An additional future work item would be to extend this analysis to include slush hydrogen propellant and more complex tank geometry.

ACKNOWLEDGMENTS

We would like to thank Dr. Jason Cassibry, Dr. Bonamente, and Dr. Miller of UAH for their assistance in developing the Exponential radiation attenuation model utilized by this paper.

REFERENCES

[1] Humble, R., *Space Propulsion Analysis and Design*, McGraw-Hill Companies, Incorporated, 1995.

[2] "J-2 Engine Fact Sheet, Saturn V News Reference," Dec. 1968.

[3] Borowski, S. K., "Nuclear Thermal Propulsion: Past Accomplishments, Present Efforts, and a Look Ahead," *Journal of Aerospace Engineering*, vol. 26, Apr. 2013, pp. 334–342.

[4] "Space Technology; Game Changing Development; Cryocooler," p. 2.

[5] McNelis, N. B., Hardy, T. L., Whalen, M. V., Kudlac, M. T., Moran, M. E., and Tomsik, T. M., "A Summary of the Slush Hydrogen Technology Program for the National Aero-Space Plane," p. 13.

[6] McCarty, R. D., J. Hord, and H. M. Roder, *Selected Properties of Hydrogen (Engineering Design Data)*, U.S. Department of Commerce/National Bureau of Standard, 1981.

[7] James R. Wertz, and Wiley J. Larson, *Space Mission Analysis and Design*, Microcosm Press and Springer, 2007.

[8] Aueron, A., Thomas, D., and Cassibry, J., "Analytical Modeling of Heat Deposition in Propellant for Nuclear Thermal Rockets," *Journal of Spacecraft and Rockets (submitted).*